Determination and photodegradation of sertraline residues in aqueous environment

(Article begins on next page)

07 January 2023

Photodegradation and transformation of sertraline in aqueous environment

Tjaša Gornik[1,2], Anja Vožič[1], Ester Heath[1,2], Jurij Trontelj[3], Robert Roškar[3], Dušan Žigon[1], Davide Vione[4], Tina Kosjek[1,2,*]

[1] *Department of Environmental Sciences, Jožef Stefan Institute, Jamova 39, Ljubljana, Slovenia*

[2] *Jožef Stefan International Postgraduate School, Jamova 39, Ljubljana, Slovenia*

[3] *Department of Biopharmacy and Pharmacokinetics, Faculty of Pharmacy, University of Ljubljana, Aškerčeva 4, Ljubljana, Slovenia*

[4] *Department of Chemistry, University of Torino, Via Pietro Giuria 5, Torino, Italy*

*Corresponding author: Jožef Stefan Institute, Jamova 39, 1000, Ljubljana, Slovenia. Tel.: +38614773288.

E-mail address: tina.kosjek@ijs.si (T. Kosjek).

ABSTRACT

Sertraline (SER) is an antidepressant of the selective serotonin reuptake inhibitor (SSRI) class that has been repeatedly reported in environmental matrices in the last decade. While the research has mostly dealt with the occurrence and toxicology of this compound, there is a lack of information pertaining to its transformation under environmental factors such as solar irradiation. The present study aimed to fill in these gaps by investigating sertraline photodegradation in laboratory scale experiments corroborated additionally by experiments on real surface water. The data, acquired by laboratory photodegradation with a medium pressure UV lamp in presence of photosensitizers or reaction quenchers, were used to predict SER phototransformation kinetics by means of the Aqueous Photochemistry of Environmentally occurring Xenobiotics (APEX) software. It was established that sertraline degrades by first-order kinetics mostly dominated by direct photolysis, while the presence of some of the reactive species including $^{\bullet}OH$, $CO_3^{\bullet}$ and $^3CDOM^*$ could further accelerate the rate of the compound's breakdown. The predicted results were validated using sertraline-spiked surface water, which was irradiated by actual sunlight, where the half-life of sertraline at around 1.4 days was estimated. Along with the photodegradation kinetics, we also identified five transformation products, three of which were successfully determined in Slovenian surface water samples. To the best of our knowledge, for two of these compounds our study represents the first report on their environmental occurrence. Overall, this work gives an insight into mechanisms of sertraline transformation in surface waters and demonstrates that photodegradation is a very important (and probably the main) transformation pathway for this contaminant.

KEYWORDS: Antidepressant; Sertraline; Water; Environment; Photodegradation; Transformation product

1. Introduction

The presence of pharmaceutical residues in environmental waters has become an established phenomenon all over the world. These compounds enter wastewater through human excretion and inappropriate disposal (Vasskog et al., 2006), especially since their removal in wastewater treatment plants (WWTPs) is often incomplete (Lajeunesse et al., 2012; Vasskog et al., 2006).

The focus of our study is the antidepressant sertraline (SER), (1S,4S)-4-(3,4-dichlorophenyl)-N-methyl-1,2,3,4-tetrahydronaphthalen-1-amine. In the year 2012 it ranked as 36th on the list of the top 200 prescription drugs dispensed in the USA (Pubchem, 2016; "Top 200 Drugs of 2012," 2016). Before entering the environment, the drug is metabolized in the liver. N-desmethylsertraline, better known as norsertraline (norSER), is the major metabolite. *In vitro* studies also report on the formation of sertraline ketone (SEK), N-hydroxy-sertraline and sertraline carbamic acid in the Phase I metabolic reactions. Glucoronidation is the main reaction of its Phase II metabolism (De Vane et al., 2002). Both the parent drug and the metabolite norSER have already been detected in the range of ng/L in surface waters (SW) and wastewaters (Golovko et al., 2014; Lajeunesse et al., 2012; Schultz et al., 2010). SER reportedly also accumulates both in sediments and aquatic organisms, affecting locomotor activity, feeding behavior, predator-prey interactions and reproduction in the latter (Hedgespeth et al., 2014a; Kwon and Armbrust, 2008; Minguez et al., 2015). The groups of Kuzmanović et al. (2016) and Osorio et al. (2016) determined SER to be one of the main emerging contaminants contributing to chronic toxic effects in four river basins in Spain.

In the environment, organic pollutants are subjected to biotic and abiotic degradation processes, among which hydrolysis, photodegradation and microbiological degradation are most common. SER is known to be hydrolytically stable and poorly biodegradable, thus

photodegradation is potentially its main natural removal process (Lam et al., 2004; US Environmental Protection Agency, 2016). By direct (DP) or indirect photolysis in aquatic environments, structural changes of the parent compound can occur, resulting in the formation of transformation products (TPs) and potentially leading to complete degradation (i.e., mineralization). The chemical structures of TPs are not necessarily identical to metabolites formed in the human body. Linking the exposure and risks related to the occurrence of parent molecules and TPs in the environment is a challenging task, of which the first steps are the definition of the exact structures of TPs and the assessment of their formation kinetics, which are amongst the principal aims of this study.

Jakimska et al. (2014) have carried out photodegradation experiments of SER under natural solar irradiation and using a xenon lamp. The impacts of matrix and pH on degradation kinetics were followed, but except for the finding that autocatalytic reactions occurred in the photodegradation mixture, there were no solid conclusions made in regards to the effects of different water matrices. To improve the lacking knowledge in this field, we aimed to assess the effect of DP as well as specific photochemical reactions on SER phototransformation kinetics and TP formation. This was achieved by measurements of photochemical reactivity on adopted laboratory systems, which were intended to measure the kinetic parameters rather than to mimic the environment. The rationale is that it is not possible to perform laboratory experiments that are representative of the environmental conditions even if natural water samples are irradiated, since there are several variables that are difficult to include in the experimental design (e.g., depth of the water column) (Bianco et al., 2015). Instead, to improve the understanding of the photochemical behaviour of natural waters, one has to model photoreactivity in deep waters and, to do so, DP quantum yields and second-order reaction rate constants are needed. With the partial exception of the processes mediated by the excited triplet states of chromophoric dissolved organic matter (^{3}CDOM*; Wenk and

Canonica, 2012), these parameters are almost independent of the experimental conditions. Therefore, the laboratory photodegradation experiments should focus on accuracy rather than on similarity to surface-water chemistry (Bodrato and Vione, 2014). For these reasons, we accomplished our research by the following steps: (*i*) laboratory measurements of SER photoreactivity parameters under UV lamps; (*ii*) photochemical modelling of SER photo-fate in shallow solutions; (*iii*) validation of our photochemical model by comparing its prediction results with the behavior of SER in river water under natural sunlight, and (*iv*) prediction of the photochemical behaviour of SER in sunlit natural water bodies. In all breakdown experiments we also followed the formation of TPs and investigated their presence in the Slovene rivers.

2. Materials and methods

2.1. Standards, chemicals and materials

The list of standards, reagents and chemicals can be found in the Supplementary material (SM), Chapter 1.1.

2.2. Preparation of standard and working solutions

The stock solutions of SER were prepared in acetonitrile (ACN) at concentrations 100 mg/L, and 500 mg/L. Considering the relatively low but non-negligible second-order reaction rate constant between ACN and $^\bullet$OH (2.2×10^7 L mol^{-1} s^{-1}; Buxton et al., 1988), the occurrence of ACN in the irradiation solutions was taken into account in the relevant kinetic models for the determination of the second-order reaction rate constant between SER and $^\bullet$OH. The stock solutions for norSER, SEK and SEI were also prepared in ACN at concentration 100 mg/L. Standard solutions of SER, norSER and SEK were stored in the dark at 4°C for 3 to 5 months, while the standard of SEI was stored in the freezer at -20°C for the longest duration of 1

month. The internal standard (IS) solutions of deuterated SER (SER-D$_3$) and deuterated bupropione (BUP-D$_9$) were provided as methanol (MeOH) solutions at the concentration of 100 mg/L and were stored at - 20°C.

2.3. Analytical method

2.3.1. Analysis of samples for the kinetics study and TP characterisation

Samples for the preliminary study of SER degradation kinetics (initial concentration of 10 µg/L) were analyzed by gas chromatography coupled to mass spectrometry (GC-MS) after appropriate sample preparation as described below. In case where no solid phase extraction (SPE) preconcentration was needed (initial concentrations of 1 mg/L and 10 mg/L), the sample was withdrawn, transferred into LC sample vial, diluted if appropriate and analyzed Quantitative trace-level analyses were performed using an ultra-high performance liquid chromatograph coupled to a hybrid quadrupole-linear ion trap mass spectrometry analyzer (UHPLC-QqLIT-MS/MS), whereas for the structural characterisation of TPs an UHPLC-hybrid quadruple time-of-flight mass spectrometer (UHPLC-QToF MS) was employed. More details on the instrumental operation are given in SM, Chapter 1.2.

We developed and optimized the sample preparation method for GC-MS determination of SER in Milli-Q (MQ) water. The final method is as follows: 200-mL samples were spiked with 50-µL of internal standard SER-D$_3$ at the concentration of 2.5 µg/L and loaded at the flow rate of 1-2 mL per minute onto Oasis HLB cartridges. The sorbent was preconditioned with 3 mL of ethyl acetate (EtAc) and 3 mL of MeOH, and equilibrated with 3 mL of MQ water. After sample loading, the sorbent was washed with 3 mL of MQ water and vacuum dried for 30 min. The analytes were eluted with 3×0.6 mL of the mixture made up of 2 % of trimethylamine (TEA) in MeOH. The extracts were nitrogen-dried at 40°C. Derivatization was performed by adding 15 µL of acetanhydride and 5 µL of pyridine to the dry extract. The

derivatization mixture was vortexed, left at room temperature for 15 min, then dried again and finally redissolved in 0.5 mL of EtAc.

2.3.2. Sample preparation of SW samples

The SW sample preparation method was the following: 250-mL of each sample was spiked with internal standard SER-D$_3$ at the final concentration of 20 ng/L, the samples were then filtered through 1.2 µm filters and 500 µL of 37 % HCl was added. The samples were loaded onto Strata XC cartridges preconditioned by 3 mL of MeOH and equilibrated by acidified MQ water (pH 2). The flow rate was 6-7 mL per minute. After loading, the matrix interferences were washed off with 4 mL of 0.1 M HCl and 2 mL of 20 % MeOH in MQ water. In the first step, the SEK fraction was eluted using 4 × 0.6 mL of MeOH. The second fraction of 3 × 0.6 mL 5 % NH$_4$OH in MeOH eluted norSER, SER, TP1 and TP2. BUP-D$_9$ was added to the first fraction of eluate at the concentration of 25 µg/L to cover for SEK instrumental analysis. The extracts were nitrogen dried at 40°C. The samples were reconstituted in 100 µL (or 200 µL for samples with higher SER concentrations – SER high) of 20% MeOH in 0.1% aqueous formic acid. The analyses were performed using UHPLC-QqLIT-MS/MS. Instrumental analysis information for each method used can be found in SM, Chapter 1.2.

2.3.4. Analytical method validation

The method performance was evaluated by estimating linearity, trueness, repeatability, sensitivity, matrix effect and SPE efficiency. The method linearity was determined from the correlation coefficient (R^2) and homoscedasticity of the matrix matched calibration curves, where the ratio of analyte to IS peak area was plotted against the concentration of analyte. Homoscedasticity was evaluated for each calibration curve following the procedure of Almeida et al. (2002): the residuals were plotted versus concentration and the F-test was

applied to check for equality of variances. In case heteroscedasticity was shown, the appropriate weighting factor was chosen on the basis of the plotted percentage relative error (% RE) versus concentration and the sum of absolute % RE to asses goodness of fit (Almeida et al., 2002). Furthermore, to avoid the saturation of SER calibration curve during UHPLC-QqLIT-MS/MS analysis, we diluted the 1 mg/L SER photodegradation samples 10 times (Table 1, Method 2).

QC samples were prepared to evaluate method repeatability and trueness (n=3). In order to confirm the trueness of our occurrence results in real SW samples, quantification was estimated by applying two methods: matrix-matched calibration and standard addition to matrices A, B and C. The method repeatability is reported as the relative standard deviation (RSD) of measurements. Trueness is expressed as the trueness error: ((calculated experimental value - spiked concentration)/spiked concentration)×100 %. Limit of quantification (LOQ) is reported as the concentration where the signal to noise (S/N) ratio was > 10 at an appropriate trueness and method repeatability (RSD < 20 % and trueness error < 20 %). SPE efficiency was determined as the ratio of the peak areas analyte/IS spiked before and after SPE, whereas IS was in any case spiked after SPE to cover for instrument signal variations. Matrix effect in SW was evaluated as the ratio of the peak area of analyte spiked into extracted matrix compared to the peak area of analyte spiked into solvent, and IS normalized.

2.4. Photodegradation experiments

2.4.1. Laboratory scale measurements for parameter modeling

Laboratory scale experiments were performed in a cylindrical glass reactor by exposing 760 mL of MQ aqueous solutions of SER to UV irradiation, at initial SER concentrations of approximately 10 µg/L and 1 mg/L (Figure S-1). A medium pressure mercury lamp (MP, 125

W, 3010/PX0686 Photochemical Reactors Ltd, London, UK) was used as the source of UV radiation. The lamp radiates predominantly at 365-366 nm, with smaller amounts at 265, 297, 303, 334 nm in the UV region and larger amounts at 404-408, 436, 546 and 577-579 nm in the visible region ("Photochemical Reactors Ltd," n.d.). A filter of borosilicate glass was used to cut off transmission below 300 nm. The intensity of the lamp was determined with ferrioxalate actinometry as 1.41×10^{-6} E s^{-1}, according to the procedure adapted from Kete et al. (2008) and Murov et al. (1993). The spectra of SER absorbance and the relative intensity spectra of the MP lamp equipped with the filter are provided in the SM (Figure S-2).

Degradation kinetics was described with the first-order degradation rate constant (k'_{SER}) and half-life ($t_{1/2}$) of SER at specified concentrations. The exposure times were adapted on the basis of the observed degradation rate. In case of UHPLC-MS/MS analysis 1-mL sub-samples were withdrawn from the same photodegradation experiment, whereas in case of the GC-MS analysis a 200-mL sample for each time point was withdrawn from an individual photodegradation experiment. Analyses were performed in duplicates. Repeatability of the photodegradation experiments was determined as the relative standard deviation (RSD) between three replicate experiments at the initial concentration of 1 mg/L and with the addition of 1mM NaNO$_3$. The RSD is reported for three time points (0, 30, 120 min).

In the experiments, we investigated the influence on degradation kinetics of pH and of radical sources or scavengers: NaNO$_3$ (1.0 mM), 2-propanol (2-P; 0.3 µM, 3.0 µM, 30 µM), NaHCO$_3$ (0.50, 1.0, 10 mM), NaH$_2$PO$_4$ (1.0, 10 mM), Rose Bengal (RB; 10 µM), anthraquinone-2-sulfonic acid sodium salt monohydrate (AQ2S; 3.0 µM). The additives were chosen based on the requirements of the modelling software (see segment 2.5 Photochemical modelling). In direct photolysis experiments, for the pH 5.0 adjustment we used acetate buffer (4 mM) and for pH 12.0 the 4 mM phosphate buffer. Along with the degradation kinetics study we followed the formation of TPs.

2.4.2. Photodegradation in surface waters

The SW solar irradiation experiments were performed in 1000 mL of SW sampled from river Gradaščica (46°02'29.4"N 14°29'16.0"E), spiked at SER initial concentrations of 50 ng/L and 1000 ng/L. The chemical parameters of the surface water were monitored before starting the experiment. The concentration of nitrite and nitrate ions, dissolved organic carbon (DOC) and chemical oxygen demand (COD) were determined using Hach reagents for water analysis (see Table S-3 for details). pH was measured with a pH meter from WTW, Wissenschaftlich-Technische Werkstätten GmbH (Weilheim, Germany) and dissolved oxygen (DO) with a HQ30d probe from Hach (Düsseldorf, Germany). The irradiation lasted for 552 hours, of which 165.9 were sun hours. The experiment was executed at 45°58'10.6"N 14°41'53.7"E. The irradiation data was collected at the closest weather station, 25 km away, where the solar hours were determined with a heliograph with a threshold between 100-150 W/m^2 of direct irradiation.

Along with the solar irradiation experiments the same matrix spiked with the same amount of SER was irradiated using UV/VIS MP Hg lamp as described in section 2.4.1. This experiment lasted for 16 h.

2.5. Photochemical modeling

The model assessment of SER photodegradation was carried out with the APEX software (Aqueous Photochemistry of Environmentally-occurring Xenobiotics), available for free as Electronic Supplementary Information of Bodrato and Vione (2014). To predict reaction kinetics in natural SW, the following input parameters are required: (*i*) substrate (SER) photoreactivity parameters including the absorption spectrum, DP quantum yield and reaction rate constants with the main photoreactive transients involved in indirect photochemistry; (*ii*) water body parameters including chemical composition (nitrite and nitrate concentration,

dissolved organic carbon, chemical oxygen demand, pH and dissolved oxygen) and water column depth. These data enable the assessment of radiation absorption by SER and the photosensitizers (NO_3^-, NO_2^- and the chromophoric dissolved organic matter, CDOM) as well as the production, scavenging and steady-state concentrations of the photogenerated transient species that include the hydroxyl ($^\bullet OH$) and carbonate ($CO_3^{\bullet -}$) radicals, singlet oxygen ($^1O_2$), as well as CDOM (chromophoric dissolved organic matter) triplet states ($^3CDOM^*$). These transients are generated by NO_3^-, NO_2^- and CDOM under sunlight irradiation, with $CO_3^{\bullet -}$ also requiring the interaction of $^\bullet OH$ with HCO_3^-/CO_3^{2-} and of $^3CDOM^*$ with CO_3^{2-} (Canonica et al., 2005; Bodrato and Vione, 2014; Vione, 2014). The standard solar spectrum used in APEX is referred to fair-weather conditions during summertime at mid latitude (Frank and Klöpffer, 1988). Because sunlight irradiance is not constant in the natural environment due to fluctuations in meteorological conditions (not included in APEX) and of diurnal and seasonal cycles, APEX uses a summer sunny day (SSD) as time unit, equivalent to fair-weather 15 July at 45° N latitude. Radiation absorption by SER, NO_3^-, NO_2^- and CDOM is calculated based on Lambert-Beer competition for sunlight irradiance (Bodrato and Vione, 2014; Braslavsky, 2007). APEX applies to well-mixed waters and gives average values of phototransformation rate constants and lifetimes over the water column, which includes the contributions of the well-illuminated surface layer and of darker water in the lower depths, where irradiance is low (Loiselle et al., 2008).

2.6 Real environmental samples

In order to confirm the presence of SER and its TPs in the environment, three six-hour composite samples were taken from three different SW (hereafter A, B and C) using an Avalanche Multi-bottle, Multi-function Sampler (Teledyne, ISCO, Lincoln, USA). The coordinates of the sampling sites, sampling dates and other parameters can be found in Table

4. The samples were prepared following the analytical method for SW and SER, norSER and SEK were quantified by UHPLC-QqLIT-MS/MS.

3. Results and discussion

3.1 Development and validation of the analytical method for SER determination in aqueous environment

Table 1 reports the validation parameters for the three developed methods: the GC-MS method (Method 1) and the UHPLC-QqLIT-MS/MS method both validated in MQ water (Method 2) and applied to laboratory samples described in segment 2.4.1, as well as the UHPLC-QqLIT-MS/MS method for SW (Method 3) used for samples from segments 2.4.2 and 2.6. Where applicable, weighting factors are also reported. The LOQ of Method 1 (GC-MS) was too high to tackle environmental levels of SER, while the UHPLC-QqLIT-MS/MS method was favoured due to its simplicity and sufficient sensitivity. Method 3 is the environmentally applicable one; it showed satisfactory repeatability and trueness and it was validated in the relevant concentration range. The trueness error and method repeatability data from the standard addition samples in SW matrices A, B and C also show that Method 3 can be successfully applied for quantifying SER and its TPs in other SW matrices (Table 1).

Table 1. Validation parameters for the three analytical methods and the results for trueness errors and method repeatability for the standard addition in matrices A, B and C.

Compound	Method (matrix)	Detection mode	Method repeatability (RSD)			Trueness error (%)			Calibration		SPE eff (%)		ME eff (%)		LOQ		Concentration range
			LOQ	LL	HL	LOQ	LL	HL	weight	R^2	LL	HL	LL	HL	S/N	(ng/L)	(ng/L)
SER	1 (MQ)	SIM	17.7	8.2	1.6	15.7	11.2	2.2	none	0.9997	70	75	/	/	∞	125	125 -1200
SER	2 (MQ)	MRM	8.9	8.6	5.5	16.9	5.1	5.6	$1/y^2$	0.9928	/	/	/	/	98.8	0.4	0.4 -100
SER	3 (SW)	MRM	13.9	6.2	6.3	14.4	3.4	6.5	$1/x^2$	0.9908	93	82	105	98	36.1	0.4	0.4 - 50
SER high			/	5.1	4.5	/	4.0	3.7	$1/x^2$	0.9940	84	96	95	118	/	/	50– 1040
norSER			10.5	5.7	5.1	5.8	1.5	1.8	$1/x^2$	0.9943	72	95	172	116	11.4	0.4	0.4 - 50
SEK			8.9	3.1	7.5	8.8	2.9	9.4	$1/x^2$	0.9892	74	74	141	185	13.8	1.0	1.0 - 50

Compound	Method (matrix)	Detection mode	Method repeatability (RSD)		Trueness error (%)	
			LL	HL	LL	HL
SER	3 (SW A)	MRM	7.7	3.4	12.3	3.8
	3 (SW B)		3.7	3.3	4.0	3.3
	3 (SW C)		5.0	5.3	11.3	5.3
norSER	3 (SW A)	MRM	12.9	6.3	10.1	6.6
	3 (SW B)		14.5	2.6	12.4	13.0
	3 (SW C)		3.6	13.4	4.8	12.6
SEK	3 (SW A)	MRM	15.0	12.0	15.6	17.2
	3 (SW B)		10.6	10.2	14.4	6.8
	3 (SW C)		12.9	8.0	17.8	5.3

Legend	Method 1 (ng/L)	Method 2 (ng/L)	Method 3 (ng/L)
LL	1000	5	5
HL	10000	50	50
LL (SER high)	/	/	50
HL (SER high)	/	/	700

13

1

3.2. SER laboratory scale photodegradation for parameter modelling

Photodegradation of SER followed pseudo-first order kinetics. The degradation constants and half-lives for different photodegradation experiments are listed in Table 2. Half-lives ranged from less than an hour to more than 2 days, depending on the reaction conditions, such as the addition of photosensitizers or quenchers, pH and SER concentration. As shown in Table 2 and Figure S-3, higher SER concentration yielded a decrease in the photodegradation rate. The experiment repeatability (RSD) was < 6.6 % for all three time points.

Table 2. First-order degradation constant (k'_{SER}) and $t_{1/2}$ of SER in the irradiated MQ solution with different additives. Where not specified, the solution pH was 7.0.

Concentration	10 μg/L		1 mg/L	
Conditions	k'_{SER} [min^{-1}]	$t_{1/2}$ [h]	k'_{SER} [min^{-1}]	$t_{1/2}$ [h]
pH 5.0 ± 0.1	< 0.0001	> 60	< 0.0001	> 60
pH 7.0 ± 0.1	0.001	11.6	0.0004	28.9
pH 12.0 ± 0.1	0.002	5.78	0.001	11.6
1 mM NaNO$_3$	0.006	1.93	0.001	11.6
1mM NaNO$_3$ + 0.5 mM NaHCO$_3$	0.007	1.65	0.004	2.89
1mM NaNO$_3$ + 1.0 mM NaHCO$_3$	0.016	0.72	0.006	1.93
1mM NaNO$_3$ + 10 mM NaHCO$_3$	0.050	0.23	0.009	1.28
10 μM RB	0.021	0.55	0.016	0.72
3.0 μM AQ2S: 1st stage	0.034	0.34	0.050	0.23
3.0 μM AQ2S: 2nd stage	0.008	1.44	0.001	11.6

3.2.1. Direct photolysis and impact of pH on the degradation constant

In order to evaluate the influence of pH on SER direct photodegradation, we performed the experiments at different pH values, e.g., at pH 5.0, pH 7.0 and pH 12.0. The pH 7.0 was chosen to reflect natural conditions, while the pH 5 and 12 were chosen to observe if the ionization of the compound influences the degradation time and kinetics. Because of the

presence of an amino group, at chosen pH the compound is either fully protonated (pH 5 and 7) or in neutral form (pH 12). The environmental relevance of this experiment is however small, since the pH of natural waters does not vary as much. The results (Table 2 and Figure S-4) proved that photodegradation is pH-dependent, resulting in fastest degradation at the alkaline pH. In agreement with the results for the other SSRI, which are all weak bases (Kwon and Armbrust, 2004, 2005a, 2005b, 2006) the degradation rate decreased with decreasing pH. We chose to perform the remaining experiments at pH 7.0 as an approximation of natural pH, while also maintaining the optimal conditions for the reagents we used. At pH 7, the calculation of the DP quantum yield of SER (see SM, Chapter 3.1) gave $\Phi_{SER} = 0.95$. This value is quite high and, when combined with the absorption of radiation by SER that is extended up to around 450 nm (Figure S-2), it suggests that the DP is likely to be a very important phototransformation process for SER in natural waters.

3.2.2. Reaction with $^{\bullet}OH$

Amongst the sources of $^{\bullet}OH$ in environmental waters, which include nitrate and nitrite ions and several organic compounds, we selected the nitrate. The reason is that it gives better estimations of the $^{\bullet}OH$ reaction rate constant than nitrite, whose quantum yield of $^{\bullet}OH$ formation varies in the solar UV range, which is not the case with nitrate. Additionally, since SER is not a phenolic compound and its aromatic rings are much more electron-poor, N-centered radicals are unlikely to react with it, in contrast with $^{\bullet}OH$ (Bedini et al., 2012a). In the experimental setup we added 1.0 mM of NO_3^-, which induced a degradation kinetics that was ideal for SER degradation monitoring. As expected, the degradation rate in the presence of $^{\bullet}OH$ radicals was notably higher as compared to the DP (Table 2). 2-Propanol (2-P) was added at final concentrations of 0.3 µM, 3.0 µM, 30 µM to the reaction mixture for determining the second-order reaction rate constant between SER and the formed $^{\bullet}OH$. 2-P
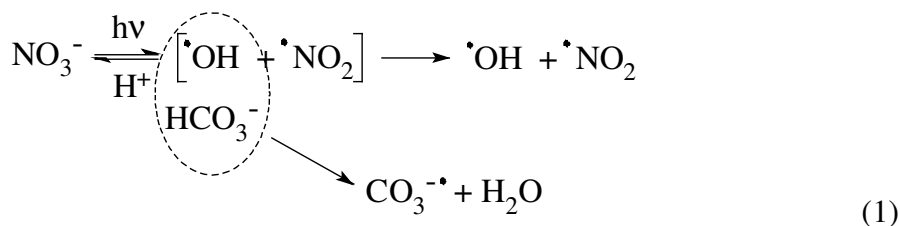
works as $^\bullet OH$ scavenger and competes with SER for $^\bullet OH$ reaction, resulting in a decrease in the SER degradation rate (Figure S-7). The kinetic model used to describe $^\bullet OH$ degradation took into account the occurrence of ACN in the system, which derived from the dilution of the SER stock solution in this solvent. The exact mechanism and calculations can be found in SM, Chapter 3.2 (reactions S1-S5) (Vione et al., 2011). The calculated reaction rate constant between SER and $^\bullet OH$ was $k_{SER+^\bullet OH} = 2 \times 10^{10}$ M^{-1} s^{-1}. The value of $k_{SER+^\bullet OH}$ indicates that the reaction between SER and $^\bullet OH$ is near diffusive control in aqueous solution.

3.2.3. Reaction with $CO_3^{\bullet-}$

The concentrations of carbonate and bicarbonate ions in the environmental waters depend on the composition of rock and soil that water flows through. Carbonates are mostly reported as the water hardness and can even exceed 1000 mg/L in ground waters (USGS, n.d.). During irradiation of natural water samples, carbonate radicals $CO_3^{\bullet-}$ are formed upon oxidation of HCO_3^-/CO_3^{2-} by $^\bullet OH$, and of CO_3^{2-} by $^3CDOM^*$ (Canonica et al., 2005). These radicals may also affect photodegradation, but they are less reactive than $^\bullet OH$ (Vione et al., 2011). To observe the effect of $CO_3^{\bullet-}$ on SER photodegradation, we added NaHCO$_3$ at final concentrations of 0.50 mM, 1.0 mM and 10 mM to the mixture containing NO$_3^-$ and SER. The nitrate photolysis yields $^\bullet OH$, which in turn produces $CO_3^{\bullet-}$ upon reaction with bicarbonate and carbonate. The proposed mechanism of reaction with SER includes reactions between all three components ($^\bullet OH$, $CO_3^{\bullet-}$ and SER) (Bouillon and Miller, 2005; Vione et al., 2011).

We observed an increase in SER photodegradation rate with increasing concentration of NaHCO$_3$ (SM, Chapter 2.2, Figure S-5, Chapter 3.3, Figure S-8), which might be compatible with a significant role played by $CO_3^{\bullet-}$ in SER photodegradation. Actually, the inorganic

carbon species HCO_3^- and CO_3^{2-} react with $^\bullet OH$ both in the solution bulk and in the solvent cage, where $^\bullet OH$ is initially formed upon nitrate photolysis as a geminate species together with $^\bullet NO_2$. The cage reaction inhibits the geminate recombination between $^\bullet OH$ and $^\bullet NO_2$, thus the formation rate of $CO_3^{\bullet -}$ in the presence of concentrated HCO_3^- / CO_3^{2-} is higher than the $^\bullet OH$ formation rate with nitrate alone (Vione et al., 2009a).

$$NO_3^- \underset{H^+}{\overset{h\nu}{\rightleftharpoons}} \left[^\bullet OH + ^\bullet NO_2 \right] \longrightarrow \, ^\bullet OH + ^\bullet NO_2$$
$$HCO_3^- \searrow$$
$$CO_3^{-\bullet} + H_2O \qquad (1)$$

It should however be noted, that the enhancement of SER photodegradation by $NaHCO_3$ could also be affected by the change of pH, depending on the fraction of undissociated compound. Namely, the pH of the solutions increased from 6.5 to 8.2 with the increasing concentration of $NaHCO_3$ additions. To measure how this change influenced the reaction rate, and in agreement with Vione et al. (2009a), we conducted experiments with phosphate ions (combination of NaH_2PO_4 and Na_2HPO_4), at the same concentrations and pH as in the $NaHCO_3$ experiments. There were no significant changes observed with the phosphate, which confirms that $CO_3^{\bullet -}$ radicals drive the degradation of SER. Thus, by being sufficiently reactive towards $CO_3^{\bullet -}$, SER will most likely undergo a similar transformation in environmental waters (Vione et al., 2009a, 2009b).

The second-order reaction rate constant between SER and $CO_3^{\bullet -}$ ($k_{SER+CO_3^{\bullet -}}$) was determined using the APEX software with the experimental concentrations of nitrate and, where relevant, bicarbonate and carbonate at the experimental pH. Moreover, we used the above value $k_{SER+^\bullet OH} = 2 \times 10^{10}$ M^{-1} s^{-1}. The acceleration of SER photodegradation in the presence of

NaHCO$_3$ could be reproduced reasonably well by assuming $k_{SER+CO_3^{\bullet-}} = 2\times10^8$ M^{-1} s^{-1} (see SM, Chapter 3.3 for additional details).

3.2.4. Reaction with $^1O_2$

$^1O_2$ is another of the reactive transient species formed in environmental waters. As the source of $^1O_2$ we used the sensitizer molecule RB. The optimal pH values for this xantene derivative range between 5 and 12, where it occurs in the dianion form and absorbs radiation at wavelengths from 450 to 600 nm, with a maximum at 548 nm. The RB reaction mechanism under irradiation enabled us to study SER degradation induced by $^1O_2$ alone. The reaction between $^1O_2$ and SER competes with thermal deactivation of $^1O_2$ (Vione et al., 2011). In agreement with our expectations, $^1O_2$ accelerated the degradation of SER as shown in Table 2. The second-order rate constant for the reaction between SER and $^1O_2$ was calculated on the basis of additional experiments with furfuryl alcohol. The reactivity of furfuryl alcohol with RB has previously been established, which enabled us to first calculate the formation rate of $^1O_2$ (Vione et al., 2011). The calculated second-order reaction rate constant was $k_{^1O_2,SER} =$ (1.3±0.2)×10^6 L mol^{-1} s^{-1}. This reaction rate constant is relatively low (e.g., one order of magnitude lower than that of diclofenac, which reacts negligibly with $^1O_2$ in the natural environment; Avetta et al., 2016). This means that the reaction between SER and $^1O_2$ may be important in laboratory experiments of RB irradiation but it is unlikely to play an important role in sunlit natural SW. The information on the exact calculations can be found in SM, Chapter 3.4.

3.2.5. Reaction with irradiated AQ2S

AQ2S was chosen because it forms a reactive triplet state (^{3}AQ2S*) under irradiation, but does not yield $^1O_2$ or $^\bullet OH$. AQ2S is here used as the CDOM proxy, since the quinones are a part of CDOM and they form reactive triplet states. The schematic of the process can be found in SM (Chapter 3.5, Figure S-9). AQ2S is usually more reactive than CDOM, and thus represents an upper limit of ^{3}CDOM* reactivity (Bianco et al., 2016; Vione et al., 2011). Bedini et al. (2012) recommended using AQ2S concentrations lower than 0.1 mM, since at higher concentrations the sensitizing process becomes negligible compared to the DP of AQ2S (Bedini et al., 2012b). Solutions containing 3.0 µM of AQ2S yielded a sufficiently high reaction rate for SER degradation. Calculation details for the second-order rate constant $k_{SER+^3AQ2S^*}$ are provided in SM, Chapter 3.5.

3.3. Photochemical modeling

Based on the calculated photoreactivity parameters of SER, namely the photolysis quantum yield ($\Phi_{SER} = 0.95$) and the second order rate constants with $^\bullet OH$ ($k_{SER+^\bullet OH} = 2\times10^{10}$ L mol^{-1} s^{-1}), $CO_3^{\bullet -}$ ($k_{SER+CO_3^{\bullet -}} = 2\times10^8$ L mol^{-1} s^{-1}), $^1O_2$ ($k_{SER+^1O_2} = (1.3\pm0.2)\times10^6$ L mol^{-1} s^{-1}) and the AQ2S triplet state, ^{3}AQ2S* ($k_{SER+^3AQ2S^*} = 7\times10^9$ L mol^{-1} s^{-1}), it was possible to model the SER phototransformation kinetics under conditions that are significant for SW. Note that $k_{SER+^3AQ2S^*}$ can be considered as an upper limit for the reaction rate constant between SER and ^{3}CDOM*, $k_{SER,^3CDOM^*}$, because ^{3}AQ2S* is generally more reactive than average ^{3}CDOM* (Avetta et al., 2016).

Figure 1 reports the modeled first-order decay constants of SER, as well as the corresponding half-lives, as a function of the dissolved organic carbon (DOC) that is a measure of the DOM

in a water body. The different processes that contribute to SER photodegradation are also highlighted.
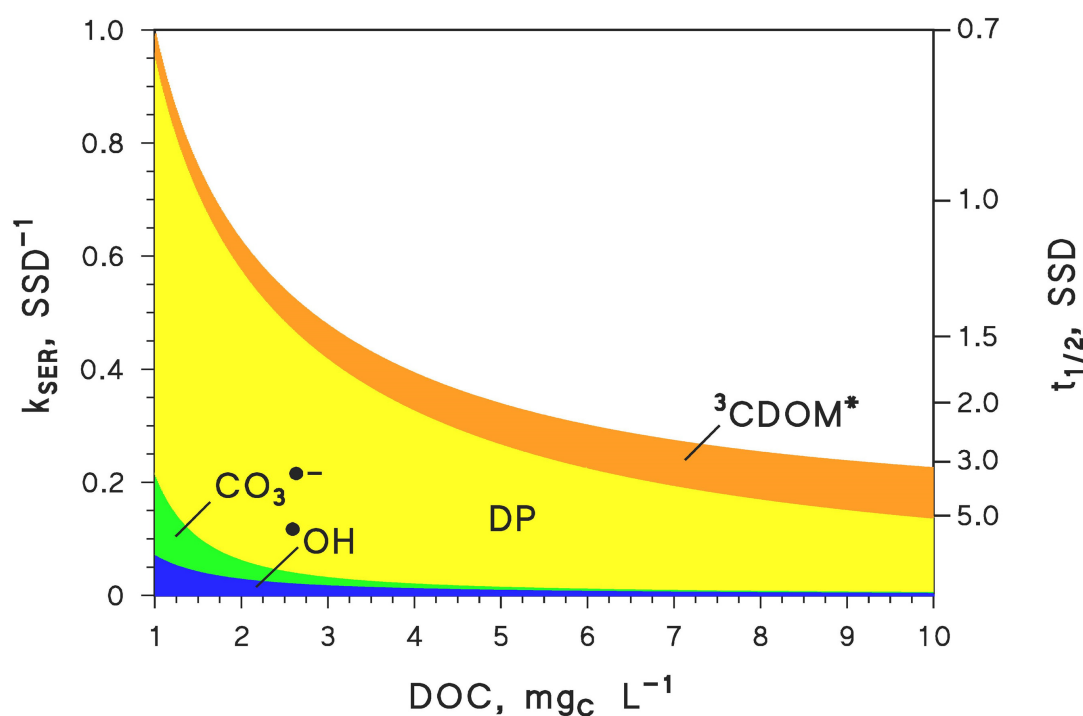

Figure 1. Modeled pseudo-first order rate constant of SER phototransformation (k_{SER}) as a function of the water DOC. The right-hand Y-axis also reports the SER half-lives. Other water conditions: 5 m depth, 0.1 mM nitrate, 1 µM nitrite, 1 mM bicarbonate, 10 µM carbonate. The steady-state $CO_3^{\bullet-}$ concentration in the modelled conditions (DOC = 1-10 mg C L^{-1}) was in the range of 10^{-16}-10^{-14} M. The different photochemical processes that account for SER photodegradation are highlighted with different colours. The time unit is the SSD (summer sunny days equivalent to 15 July at 45°N latitude).

The figure shows that, for a water depth of 5 m, the photodegradation of SER would be dominated by the DP. The reactions with $^\bullet OH$ and $CO_3^{\bullet-}$ would play a secondary role. The highlighted role of $^3CDOM^*$ is referred to $k_{SER,^3CDOM^*} = k_{SER,^3AQ2S^*}$, and it constitutes an upper limit for the importance of the process. The lower limit is obtained under the hypothesis that the $^3CDOM^*$ process is unimportant. To get an insight into the relevant range of variation, the half-life of SER with DOC = 10 mg C/L would vary from 3 days with $k_{SER,^3CDOM^*} = k_{SER,^3AQ2S^*}$, to 5 days by excluding the $^3CDOM^*$ process. Note that an increase of the DOC is expected to inhibit the reactions with $^\bullet OH$ and $CO_3^{\bullet-}$, because DOM is a key scavenger of both radical species. Increasing DOC also inhibits the DP, because the CDOM would compete with SER for sunlight irradiance. In contrast, the $^3CDOM^*$ reactions would be enhanced at high DOC because of elevated levels of CDOM that is the immediate $^3CDOM^*$ precursor (Avetta et al., 2016).

3.4. Identification of TPs and their formation profiles

3.4.1 Peak detection, identity confirmation and formation profiles

Figure S-10 in the SM shows the extracted ion chromatograms of a sample treated with RB and irradiated for 105 min. There are evident chromatographic peaks of the residual SER at 3.80 min, and of three TPs, i.e. nor-SER at 3.84 min, SEI at 3.54 min and SEK at 5.14 min. Each TP was defined by three MRM transitions (Table S-1) and the retention time matching with standards. Furthermore, we detected two additional compounds with chromatographic peaks at t_R 3.29 min and t_R 3.53 min that underwent the same transition as SEK (MRM 291>238), as shown in Figure S-10 (D) and Figure 2. The compounds TP1 and TP2 were absent in the control samples, thus we presumed them to be TPs of SER.
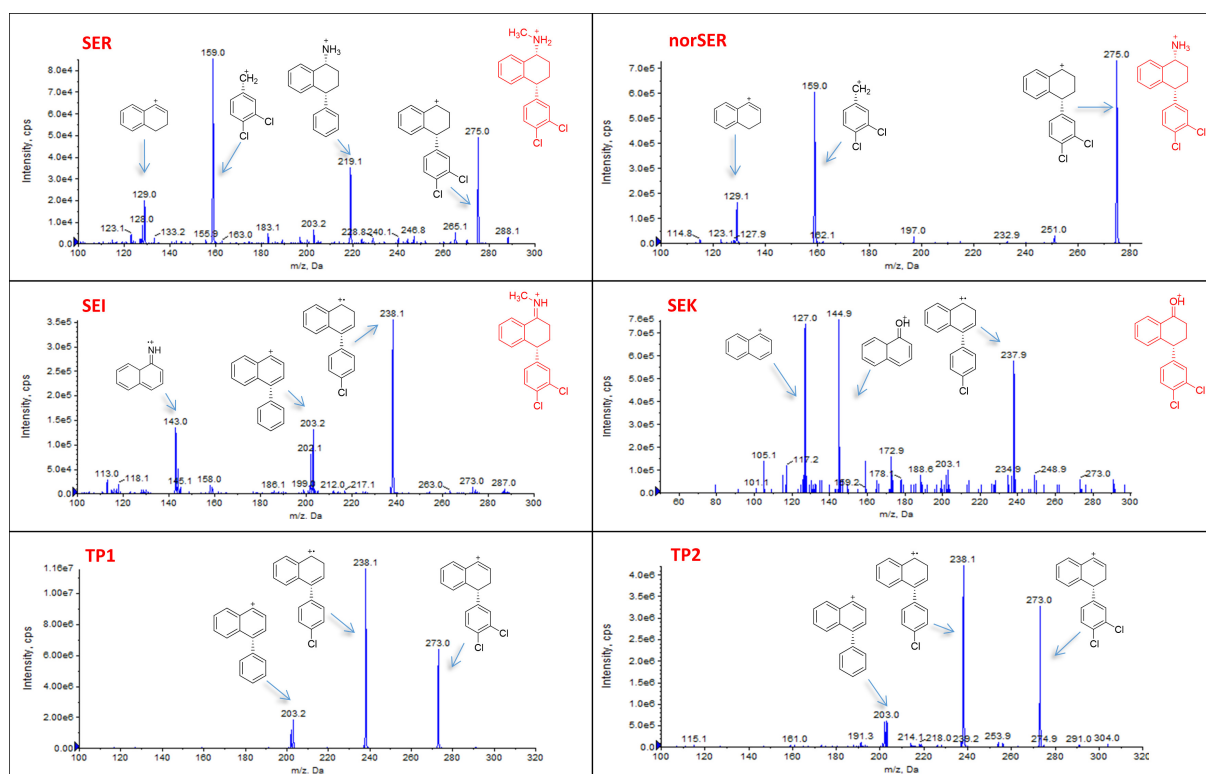
Figure 2: Enhanced product ion MS spectra of SER (top left), nor-SER (top right), SEI (middle left), SEK (middle right), TP1 (bottom left), and TP2 (bottom right) and the proposed chemical structures assigned to the fragment ions.

The formation of SEI, norSER, SEK, TP1 and TP2 was monitored over time in photodegradation experiments (direct photolysis, $NaNO_3$, $NaNO_3$ + $NaHCO_3$, RB, AQ2S, see section 2.4.1.) at SER initial concentration of 1 mg/L. The graphs showing TP formation are presented in the SM, Figures S-11 to S-19. The formation of SEI has already been proposed in the photodegradation study by Jakimska et al. (2014), and by Shen et al. (2011) in the dark reaction with the TetraAmido Macrocyclic Ligand (TAML) activator. In our experiments the formation of SEI took place instantly, i.e., at the very beginning of the irradiation experiments, though it was shown that the compound did not occur as a product of simple hydrolysis. Presumably, SEI was formed during the time lapse when the UV lamp was still heating up to achieve its full irradiation intensity. The abundance of SEI generally decreased

during the course of the experiments, except in the case of the reaction with AQ2S, which suggests that SEI may also be a product of triplet-sensitized SER degradation. SEI showed instability in water solutions, even degrading during the SPE sample preparation, which might explain its absence in real SW samples. Along with the fact that SEI clearly underwent fast degradation during the irradiation experiments (see SM, Figures S-11 to S-19), it is believed that SEI is unlikely to be a persistent TP of SER. NorSER is a metabolite of SER, but it has also been found in the reaction of SER with the TAML activator (Shen et al., 2011), whereas Jakimska et al. (2014) have not reported its formation in their photodegradation study. In our experiments, norSER was formed in all cases, except when only $NaNO_3$ ($^\bullet OH$ reaction) was added. SEK formation was observed in most cases, except for reactions with $NaNO_3$, AQ2S or upon direct photolysis at pH 5.0. Its formation was already reported by Jakimska et al. (2014) and by Shen et al. (2011). We detected TP2 only in the photodegradation reactions with triplet states (AQ2S) and $^1O_2$ (RB), while TP1 was observed during all of the experiments. The concentration of TP1 showed a gradual increase in the irradiation experiments, except in the case of AQ2S, where it reached a plateau after 15 min irradiation. In any case, the AQ2S kinetics of TP formation is very specific (Figure S-19) and is probably the result of two-stage degradation kinetics of SER.

3.4.2 Identification of TP1 and TP2

Structural elucidation of TP1 and TP2 was performed by the UHPLC-QToF MS analysis with main results gathered in Table S-2 and Figure S-20 in SM. Three main peaks were detected at 3.06 min (TP1), 3.22 min (TP2) and 3.56 min (SER), showing the same elution order on the C-18 column as in case of the UHPLC-QqLIT-MS/MS analysis. SER showed its protonated molecular ion at $[M+H]^+$ 306.0816, from which its elemental formula $C_{17}H_{17}NCl_2$ was calculated. An isotope signal at m/z 308.0810 at about 30% of the parent mass height

confirmed the presence of two Cl ions in the structure. The fragment ion observed at *m/z* 275 resulted from the loss of CH_3NH_2 and *m/z* 159 from the further loss of the tetralin ring.

For the compounds TP1 and TP2 the protonated molecule was observed at $[M+H]^+$ 322.0765, corresponding to the elemental formula $C_{17}H_{18}NOCl_2$. This means than an additional oxygen atom is incorporated into SER structure. In TP1 the most prominent fragment ion observed was *m/z* 304 formed after the loss of H_2O, while in TP2 smaller fragments at *m/z* 304 and *m/z* 291 were detected corresponding to the subsequent cleavages of H_2O and CH_3NH_2. Both TPs showed *m/z* 273, which is 2Da less than the analogous fragment ion of SER (*m/z* 275), suggesting a double bond formed during the fragmentation of the TPs. Corresponding fragmentation was previously suggested by Li et al. (2013) for TPs formed during incubation of SER in three types of agricultural soil with and without the addition on biosolids. In agreement with this report we propose the formation of hydroxysertraline with three possible placements of the OH group, making TP1 and TP2 constitutional isomers.

3.5. SW water irradiation

The lab scale photodegradation of SER in SW was carried out under both the lamp and natural sunlight. The photodegradation due to solar irradiation was two to three times slower (in solar hours) than the lab scale experiments, which was expected due to the difference in the overall irradiation energy that the samples received (Table 3).

Table 3. Degradation k'_{SER} and $t_{1/2}$ of solar and laboratory scale irradiation experiments in SW.

SER concentration [ng/L]	Type of irradiation	Units	k'_{SER} [min^{-1}]	$t_{1/2}$ [h]
50	MP lamp	hours	0.0049	2.36
	solar	hours	0.0003	34.7
	solar	solar hours	0.0012	9.33
1000	MP lamp	hours	0.0032	3.58
	solar	hours	0.0005	31.8
	solar	solar hours	0.0019	5.94

The predicted half-time for SER photodegradation, following our model at DOC concentration 4.14 mg/L as per the irradiated SW sample should be around 2 SSD. From our experimental data, the degradation lifetime is estimated at around 1.3-1.4 days (31.8 - 34.7 h), in good agreement with model predictions. The main reasons for the relatively small discrepancy are probably the difference in the irradiation energy received, pH, the column-depth bias and the fact that the SW collected was not sterile. Therefore, some biodegradation could have occurred, which is suspected based on the 37 % decrease of SER within the 1-month control study (SM, Figure S-21).

We observed that four TPs (list which ones) were formed during the SW irradiation experiments. Based on the trend in the Hg-lamp experiments and the observed maximum in the solar irradiated samples (Figure 3), we may have missed the peak concentrations of norSER and SEK during the first week of irradiation. In addition to norSER and SEK, TP1

was formed in both solar and lab scale experiments, but since there is no reference standard available for this compound, we cannot report its concentration in the figures.
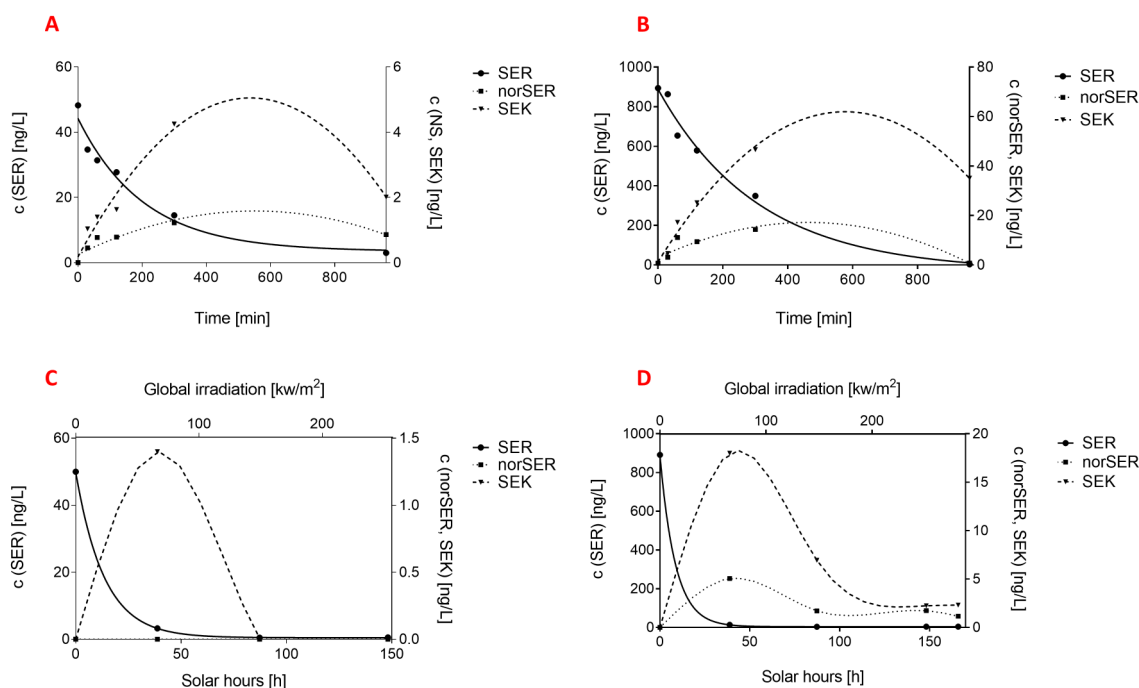

Figure 3. Photodegradation of SER and TP formation in SW at 50 ng/L (A) and 1 mg/L (B) under the medium-pressure Hg lamp and at 50 ng/L (C) and 1 mg/L (D) under sunlight.

3.6. Real surface water samples

As can be seen in Table 4, SER was detected in SW A and C. Additionally, we determined norSER and SEK in SW C. In the same sample also TP1 was identified, but not quantified due to the absence of its reference standard. TP2 was not detected, whereas possible reasoning for the absence of SEI (instability) is given in the previous segment. Altogether, we confirmed the presence of three out of five identified TPs in the environment. To the best of our

knowledge, the environmental occurrence of TP1 and SEK is reported herein for the first time. The highest concentrations of SER and TPs were detected in SW C. This finding is not surprising when taking into account that SW C flows in the region of Slovenia having the highest reported percentage of patients prescribed with SER (NIJZ, 2018), while its flow is smaller when compared to the those of the rivers SW A and SW B. Overall, while norSER and SEK may also be SER metabolites, TP1 should be significantly produced by photochemical processes, both direct and indirect.

Table 4. Sampling details, determined concentrations of SER, norSER and SEK, and qualitative determination of TP1 and TP2 in SW A, B and C.

SW	Sampling data				c [ng/L]			Screening	
	Sampling location	Sampling date	pH	DO [mg/L]	SER	norSER	SEK	TP 1	TP 2
A	46°04'10.7"N 14°37'58.6"E	16.10.2018	7.22	10.04	0.51 ± 0.16	< LOQ	< LOQ	ND	ND
B	46°06'31.7"N 14°36'41.8"E	17.10.2018	7.84	8.91	< LOQ	< LOQ	< LOQ	ND	ND
C	46°07'49.5"N 15°02'07.7"E	18.10.2018	7.82	9.10	9.28 ± 0.69	1.77 ± 0.14	1.43 ± 0.26	identified	ND

ND – not detected

4. Conclusions

- Both DP and indirect photodegradation contribute to SER photo-induced degradation, with indirect photodegradation playing a role at higher concentrations of senzitizers present.

- The degradation kinetics of SER is pseudo-first order. The rate of degradation is influenced by pH, where the protonated SER is more photochemically stable than its neutral form.

- This is the first report on formation of norSER during photodegradation under conditions that are significant for SW. While the formation of TP1 and TP2 was before suggested in soil samples, we proved that they form also in the aqueous environment.

- Solar degradation experiments confirmed the results obtained by photochemical modelling, which suggested that the SER half-life might range from < 1 day to about 3-5 days, depending on water conditions.

- The presence of SER and three of its TPs in the aqueous environment was confirmed.

Overall, this study brings a substantial insight into the photochemical fate of the antidepressant SER in the aquatic environment, but there remain several knowledge gaps on its environmental fate. One example is its unrecognized biological breakdown; yet even more far-reaching is the general issue on how to improve the determination of the compound's unknown TPs in the environment, i.e., how to make the "nontarget analysis more targeted".

Acknowledgements

References

Almeida, A.., Castel-Branco, M.., Falcão, A.., 2002. Linear regression for calibration lines revisited: weighting schemes for bioanalytical methods. J. Chromatogr. B 774, 215–222. https://doi.org/10.1016/S1570-0232(02)00244-1

Avetta P., Fabbri D., Minella M., Brigante M., Maurino V., Minero C., Pazzi M., Vione D., 2016. Assessing the phototransformation of diclofenac, clofibric acid and naproxen in surface waters: Model predictions and comparison with field data, Water Res., 105, 383-394.

Bedini, A., De Laurentiis, E., Sur, B., Maurino, V., Minero, C., Brigante, M., Mailhot, G., Vione, D., 2012b. Phototransformation of anthraquinone-2-sulphonate in aqueous solution. Photochem. Photobiol. Sci. 11, 1445. https://doi.org/10.1039/c2pp25111f

Bedini, A., Maurino, V., Minero, C., Vione, D., 2012a. Theoretical and experimental evidence of the photonitration pathway of phenol and 4-chlorophenol: A mechanistic study of environmental significance. Photochem Photobiol Sci 11, 418–424. https://doi.org/10.1039/C1PP05288H

Bianco, A., Fabbri, D., Minella, M., Brigante, M., Mailhot, G., Maurino, V., Minero, C., Vione, D., 2015. New insights into the environmental photochemistry of 5-chloro-2-(2,4-dichlorophenoxy)phenol (triclosan): Reconsidering the importance of indirect photoreactions. Water Res. 72, 271-280.

Bianco, A., Fabbri, D., Minella, M., Brigante, M., Mailhot, G., Maurino, V., Minero, C., Vione, D., 2016. Photochemical transformation of benzotriazole, relevant to sunlit surface waters: Assessing the possible role of triplet-sensitised processes. Sci. Total Environ. 566–567, 712–721. https://doi.org/10.1016/j.scitotenv.2016.05.119

Bodrato, M., Vione, D., 2014. APEX (Aqueous Photochemistry of Environmentally occurring Xenobiotics): a free software tool to predict the kinetics of photochemical processes in surface waters. Environ. Sci. Process. Impacts 16, 732–40. https://doi.org/10.1039/c3em00541k

Bouillon, R.-C., Miller, W.L., 2005. Photodegradation of Dimethyl Sulfide (DMS) in Natural Waters: Laboratory Assessment of the Nitrate-Photolysis-Induced DMS Oxidation. Environ. Sci. Technol. 39, 9471–9477. https://doi.org/10.1021/es048022z

Braslavsky, S.E., 2007. Glossary of terms used in photochemistry, 3rd edition (IUPAC Recommendations 2006). Pure Appl. Chem. 79, 293–465. https://doi.org/10.1351/pac200779030293

Buxton, G. V., Greenstock, C. L., Helman, W. P., Ross, A. B., 1988. Critical review of rate constants for reactions of hydrated electrons, hydrogen atoms and hydroxyl radicals ($^{\bullet}$OH/O$^{\bullet-}$) in aqueous solution. J. Phys. Chem. Ref. Data 17, 1027-1284.

Canonica, S., Kohn, T., Mac, M., Real, F. J., Wirz, J., Von Gunten, U., 2005. Photosensitizer method to determine rate constants for the reaction of carbonate radical with organic compounds. Environ. Sci. Technol. 39, 9182-9188.

De Vane, C.L., Liston, H.L., Markowitz, J.S., 2002. Clinical pharmacokinetics of sertraline. Clin. Pharmacokinet. 41, 1247–1266.

Frank, R., Klöpffer, W., 1988. Spectral solar photon irradiance in Central Europe and the adjacent North Sea. Chemosphere 17, 985–994. https://doi.org/10.1016/0045-6535(88)90069-0

Golovko, O., Kumar, V., Fedorova, G., Randak, T., Grabic, R., 2014. Seasonal changes in antibiotics, antidepressants/psychiatric drugs, antihistamines and lipid regulators in a wastewater treatment plant. Chemosphere 111, 418–426. https://doi.org/10.1016/j.chemosphere.2014.03.132

Hedgespeth, M.L., Nilsson, P.A., Berglund, O., 2014a. Ecological implications of altered fish foraging after exposure to an antidepressant pharmaceutical. Aquat. Toxicol. 151, 84–87. https://doi.org/10.1016/j.aquatox.2013.12.011

Jakimska, A., Kaszynska M., 2014. Environmental Fate of Two Psychiatric Drugs, Diazepam and Sertraline: Phototransformation and Investigation of their Photoproducts in Natural Waters. J. Chromatogr. Sep. Tech. 05. https://doi.org/10.4172/2157-7064.1000253

Kete, M., 2008. The development of pilot water purification system based on TiO_2 photocatalysis "Razvoj pilotnega sistema za čiščenje vode na principu TiO_2 fotokatalize". Univerza v Novi Gorici.

Kuzmanović, M., López-Doval, J.C., De Castro-Català, N., Guasch, H., Petrović, M., Muñoz, I., Ginebreda, A., Barceló, D., 2016. Ecotoxicological risk assessment of chemical pollution in four Iberian river basins and its relationship with the aquatic macroinvertebrate community status. Sci. Total Environ. 540, 324–333. https://doi.org/10.1016/j.scitotenv.2015.06.112

Kwon, J.-W., Armbrust, K.L., 2008. Aqueous Solubility, n-Octanol–Water Partition Coefficient, and Sorption of Five Selective Serotonin Reuptake Inhibitors to Sediments and Soils. Bull. Environ. Contam. Toxicol. 81, 128–135. https://doi.org/10.1007/s00128-008-9401-1

Kwon, J.-W., Armbrust, K.L., 2006. Laboratory persistence and fate of fluoxetine in aquatic environments. Environ. Toxicol. Chem. 25, 2561–2568. http://doi.org/10.1897/05-613R.1

Kwon, J.-W., Armbrust, K.L., 2005a. Degradation of citalopram by simulated sunlight. Environ. Toxicol. Chem. 24, 1618–1623. http://doi.org/10.1897/04-522R.1

Kwon, J.-W., Armbrust, K.L., 2005b. Photo-isomerization of fluvoxamine in aqueous

solutions. J. Pharm. Biomed. Anal. 37, 643–648.

https://doi.org/10.1016/j.jpba.2004.09.057

Kwon, J.-W., Armbrust, K.L., 2004. Hydrolysis and photolysis of paroxetine, a selective

serotonin reuptake inhibitor, in aqueous solutions. Environ. Toxicol. Chem. 23, 1394–

1399. http://doi.org/10.1897/03-319

Lajeunesse, A., Smyth, S.A., Barclay, K., Sauvé, S., Gagnon, C., 2012. Distribution of

antidepressant residues in wastewater and biosolids following different treatment

processes by municipal wastewater treatment plants in Canada. Water Res. 46, 5600–

5612. https://doi.org/10.1016/j.watres.2012.07.042

Lam, M.W., Young, C.J., Brain, R.A., Johnson, D.J., Hanson, M.A., Wilson, C.J., Richards,

S.M., Solomon, K.R., Mabury, S.A., 2004. Aquatic persistence of eight

pharmaceuticals in a microcosm study. Environ. Toxicol. Chem. 23, 1431–1440.

http://doi.org/10.1897/03-421

Li, H., Sumarah, M.W., Topp, E., 2013. Persistence and dissipation pathways of the

antidepressant sertraline in agricultural soils. Sci. Total Environ. 452–453, 296–301.

https://doi.org/10.1016/j.scitotenv.2013.02.080

Loiselle, S.A., Azza, N., Cozar, A., Bracchini, L., Tognazzi, A., Dattilo, A., Rossi, C., 2008.

Variability in factors causing light attenuation in Lake Victoria. Freshw. Biol. 53,

535–545. https://doi.org/10.1111/j.1365-2427.2007.01918.x

Minguez, L., Ballandonne, C., Rakotomalala, C., Dubreule, C., Kientz-Bouchart, V., Halm-

Lemeille, M.-P., 2015. Transgenerational Effects of Two Antidepressants (Sertraline

and Venlafaxine) on *Daphnia magna* Life History Traits. Environ. Sci. Technol. 49,

1148–1155. https://doi.org/10.1021/es504808g

Murov, S.L., Carmichael, I., Hug, G.L., 1993. Handbook of Photochemistry, Second Edition. CRC Press.

National Institute of public health (NIJZ), 2018. Poraba ambulantno predpisanih zdravil v Sloveniji v letu 2017. Ljubljana.

Osorio, V., Larrañaga, A., Aceña, J., Pérez, S., Barceló, D., 2016. Concentration and risk of pharmaceuticals in freshwater systems are related to the population density and the livestock units in Iberian Rivers. Sci. Total Environ. 540, 267–277. https://doi.org/10.1016/j.scitotenv.2015.06.143

Photochemical Reactors Ltd, n.d. URL http://www.photochemicalreactors.co.uk/html/immersion-well-reactors.html (accessed 11.8.17).

Pubchem, 2016. Sertraline, $C_{17}H_{17}Cl_2N$ - PubChem. URL https://pubchem.ncbi.nlm.nih.gov/compound/sertraline#section=Names-and-Identifiers (accessed 7.3.16).

Shen, L. Q., Beach, E. S., Xiang, Y., Tshudy, D. J., Khanina, N., Horwitz, C. P., Biert, M. E., Collins, T. J. (2011). Rapid, Biomimetic Degradation in Water of the Persistent Drug Sertraline by TAML Catalysts and Hydrogen Peroxide. Environmental Science & Technology, 45(18), 7882–7887. https://doi.org/10.1021/es201392k

Schultz, M.M., Furlong, E.T., Kolpin, D.W., Werner, S.L., Schoenfuss, H.L., Barber, L.B., Blazer, V.S., Norris, D.O., Vajda, A.M., 2010. Antidepressant pharmaceuticals in two US effluent-impacted streams: occurrence and fate in water and sediment, and selective uptake in fish neural tissue. Environ. Sci. Technol. 44, 1918–1925. http://doi.org/10.1021/es9022706

Top 200 Drugs of 2012, 2016. URL

http://www.pharmacytimes.com/publications/issue/2013/july2013/top-200-drugs-of-

2012 (accessed 7.3.16).

US Environmental Protection Agency, 2016. Final Report, The Environmental Occurrence,

Fate, and Ecotoxicity of Selective Serotonin Reuptake Inhibitors (SSRIs) in Aquatic

Environments, Research Project Database. URL

https://cfpub.epa.gov/ncer_abstracts/index.cfm/fuseaction/display.highlight/abstract/1

755/report/F (accessed 7.3.16).

USGS, n.d. Water-Quality Information: Water Hardness and Alkalinity, URL

https://water.usgs.gov/owq/hardness-alkalinity.html (accessed 5.7.17).

Vasskog, T., Berger, U., Samuelsen, P.-J., Kallenborn, R., Jensen, E., 2006. Selective

serotonin reuptake inhibitors in sewage influents and effluents from Tromsø, Norway.

J. Chromatogr. A 1115, 187–195. https://doi.org/10.1016/j.chroma.2006.02.091

Vione, D., 2014. A test of the potentialities of the APEX software (Aqueous Photochemistry

of Environmentally occurring Xenobiotics). Modelling the photochemical persistence

of the herbicide cycloxydim in surface waters, based on literature kinetic data.

Chemosphere 99, 272–275. https://doi.org/10.1016/j.chemosphere.2013.10.078

Vione, D., Khanra, S., Man, S.C., Maddigapu, P.R., Das, R., Arsene, C., Olariu, R.-I.,

Maurino, V., Minero, C., 2009a. Inhibition vs. enhancement of the nitrate-induced

phototransformation of organic substrates by the •OH scavengers bicarbonate and

carbonate. Water Res. 43, 4718–4728. https://doi.org/10.1016/j.watres.2009.07.032

Vione, D., Maddigapu, P.R., De Laurentiis, E., Minella, M., Pazzi, M., Maurino, V., Minero,

C., Kouras, S., Richard, C., 2011. Modelling the photochemical fate of ibuprofen in

surface waters. Water Res. 45, 6725–6736.

https://doi.org/10.1016/j.watres.2011.10.014

Vione, D., Maurino, V., Minero, C., Carlotti, M.E., Chiron, S., Barbati, S., 2009b. Modelling the occurrence and reactivity of the carbonate radical in surface freshwater. Comptes Rendus Chim. 12, 865–871. https://doi.org/10.1016/j.crci.2008.09.024

Wenk, J., Canonica, S., 2012. Phenolic antioxidants inhibit the triplet-induced transformation of anilines and sulfonamide antibiotics in aqueous solution. Environ. Sci. Technol. 46, 5455-5462.